A Novel Receiver for FHMA Systems

Chen Jiang and Jiangzhou Wang, *Senior Member, IEEE*

***Abstract*—A novel FH/MFSK receiver with additional partial correlators is proposed by means of side information for asynchronous frequency-hopping multiple-access (FHMA) systems in the presence of Rayleigh fading. Performance analysis is carried out and compared for both the novel and conventional receivers. One hop per symbol and Reed–Solomon (RS) coding are used in the FHMA systems. It is shown that the novel receiver performs much better than the conventional receiver for a wide range of signal to noise ratio. The capacity of the FHMA system with novel receivers is almost as twice as that of the system with conventional receivers.**

***Index Terms*—Fading channels, frequency hopping, multi-access.**

I. Introduction

THE increasing demand for bandwidth in mobile communication services has fueled the search for higher capacity wireless systems. This search has created a commercial interest in spread-spectrum (SS) systems which offer significant capacity improvement in multiple access (MA) systems. Although a great deal of emphasis has been placed on direct sequence spread spectrum (DS/SS), recent developments in frequency-hopping multiple-access (FHMA) technology [1]–[11] have resulted in commercial applications such as mobile cellular communications, personal communications and wireless local area networks (LANs) . On the other hand, FHMA systems have been considered for a variety of military applications due to their frequency diversity and resistance to the near-far problem [12].

In FHMA systems, each active user transmits M-ary frequency shift keying (MFSK) modulated signals with independent hopping patterns over a given common spread bandwidth. Therefore, detection of symbol from the reference transmitter is affected by the signals from other nonreference users transmitting simultaneously at the same frequency. This phenomenon is known as a "hit". The performance measure that one may be interested in is the number of users for which communication is possible with the error probability below a certain desired value. This is called the achievable region. This performance measure allows one to determine the maximum number of users that can simultaneously transmit.

In this paper, we present a novel receiver with additional correlators and an noncoherent MFSK demodulator, which offers the performance improvement without incurring much of the implementation complexity. In FHMA systems, synchronous hopping of all users is useful to mitigating the effect of multiple-access interference under some special conditions, but it is technically very difficult to achieve this kind of synchronization in practice, specially in decentralized systems. Therefore, our system is assumed to operate in an asynchronous manner. That is, the transmission times between various users are not coordinated. When the observed signal is hit, it is expected to utilize the delay between the desired signal and interference signals of nonreference users to reduce the effect of interference. In order for the error probability of the receiver to be below a certain desired value over Rayleigh channel and further mitigating the effect of multiple-access interference, the Reed–Solomon (RS) coding with fixed rate is considered because of its good burst error-correcting capability.

In Section II, we establish the system model and present the construction of the novel FH/MFSK receiver. Section III concentrates on the analysis of bit error rate of the novel MFSK receiver with Rayleigh fading. Numerical results and comparison between the novel and conventional receivers are given in Section IV. Finally, this paper is concluded in Section V.

II. System Model

Let K denote the number of active transmitter-receiver pairs of the FHMA system under consideration. The transmitter for the kth user ($1 \le k \le K$) consists of the following parts:

- A Reed–Solomon encoder, which converts block of l source symbols into a codeword of n coded symbols. The sequence of coded symbols is represented as $b_k(t)$; the λth coded symbol of $b_k(t)$ has amplitude $b_k^{(\lambda)}$, taking values from the set $\{0, 1, \ldots, M-1\}$. The coded symbol rate R_S is given by $R_S = R_b/\log_2 M$, where R_b denotes the rate of the coded bits. The information bit rate R_i (i.e., the rate of source bits) is given by $R_i = R_b(l/n)$, where l/n is the rate of the RS code.
- A MFSK modulator, which translates each coded symbol $b_k^{(\lambda)}$ into a sinusoidal tone with frequency $f_c + b_k^{(\lambda)}2\Delta$, where 2Δ stands for the frequency spacing among adjacent MFSK tones. In order that these tones are orthogonal, $2\Delta T_S$ must be an integer, where $T_S = 1/R_S$ is the symbol duration.
- A frequency hopper, operating at only one hop per coded symbol. Q is defined as the number of total hopping frequencies. The frequency hopper translates the signal symbol into a sinusoidal tone with frequency $f_k^{(\lambda)} + b_k^{(\lambda)}2\Delta$, where $f_k^{(\lambda)}$ is first-order Markov sequence so that two consecutive hopping frequencies are always different. This assumption guarantees that two adjacent hops of the reference user are not hit together by an nonreference user. It is assumed that the hits due to multiple-access interference are independent from hop to hop. In fact, Hegde and Stark [4] has proven that though the hits exhibit an underlying

Manuscript received March 11, 2001; revised October 15, 2001 and November 21, 2001.

The authors are with the Department of Electrical and Electronic Engineering, The University of Hong Kong, Hong Kong (e-mail: jwang@eee.hku.hk).

Digital Object Identifier 10.1109/TVT.2002.800640

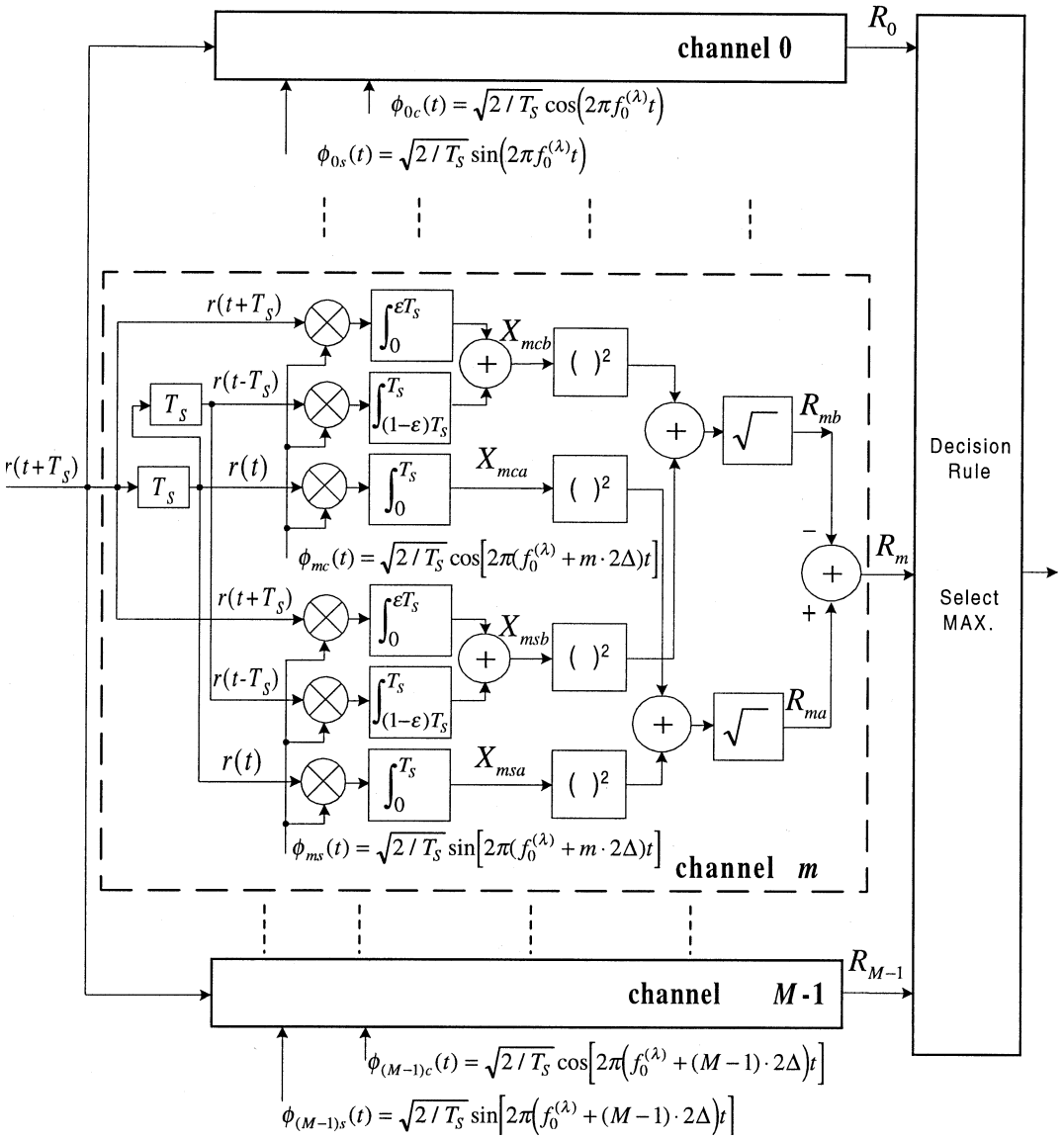

Fig. 1. A detail block diagram of MFSK receiver with partial correlation, where is the delay element.

Markov structure, the independence assumption is quit accurate. When the RS coding is employed, the minimum system bandwidth is given by

$$W_{\text{Total}} = R_i Q\left(\frac{M}{\log_2(M)}\right)\left(\frac{n}{l}\right) \tag{1}$$

It is assumed that the channel between any transmitter and the reference receiver is a slow Rayleigh fading channel, where "slow" means that the signal amplitude can be assumed to be fixed in one symbol.

Corresponding to the transmitter, the receiver consists of a frequency dehopper, a noncoherent MFSK demodulator, a hard decision device and a Reed–Solomon (RS) decoder. To reduce the effect of multi-access interference (MAI), a number of partial correlators in the demodulator of novel receiver are used. Fig. 1 makes use of information extracted from the previous and the next symbol interval to improve the robustness to MAI of the decision related to the present symbol interval. In Fig. 1, R_{ma} is the conventional square law detector output and R_{mb} is the square law detector output for the earlier and later side information. The decision variable R_m is equal to $R_{ma} - R_{mb}(R_m = R_{ma} - R_{mb})$. Since the desired signal component is only contained in R_{ma} and the MAI tones generally are included in both R_{ma} and R_{mb}, the MAI in R_m is reduced by the subtraction. In order to use the side information in an optimum way, the parameter ε is very important to balance the advantage of depressing MAI against the disadvantage of additional white noise. When $\varepsilon = 0$, the proposed receiver reduces to the conventional FH/MFSK receiver (Fig. 2). Assuming that the user "0" is the reference user, the received signal is the sum of the reference signal, multiple-access interference and channel noise, given by

$$\begin{aligned} r(t) =& \beta_0 \sin\left[2\pi\left(f_0^{(\lambda)} + b_0^{(\lambda)}\cdot 2\Delta\right)t + \theta_0\right] \\ &+ \sum_{k=1}^{K-1}\beta_k \sin\left[2\pi\left(f_k^{(\lambda)} + b_k^{(\lambda)}\cdot 2\Delta\right)\right. \\ &\left.\cdot(t-\tau_k) + \theta_k\right] + n(t) \end{aligned} \tag{2}$$

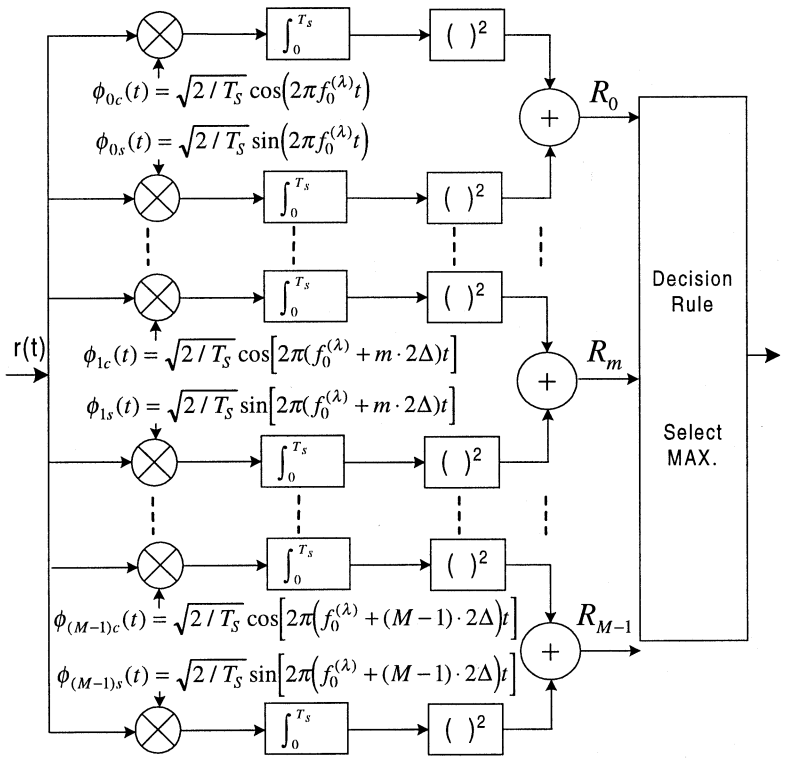

Fig. 2. Conventional MFSK nocoherent receiver.

where the first term represents the reference signal (or desired signal). The remaining terms consist of the multiple-access interference from nonreference users and white noise with two-sided power spectral density of height $N_0/2$. The phases θ_0 and θ_k are independent random variables uniformly distributed in [0, 2π). β_0 and β_k are the signal amplitudes of reference and nonreference users, respectively, and are independent Rayleigh random variables with the second moment $E\left[\beta_0^2\right] = 2P_S$ and $E\left[\beta_k^2\right] = 2P_k$, respectively. For simple analysis, we assume that all signals are received with the same average power $P_k = P_S$. Furthermore, we assume that the delays (τ_k) of nonreference signals are random variables. During the λth signal symbol, the signal frequency is $f_0^{(\lambda)} + b_0^{(\lambda)} \cdot 2\Delta$ and the corresponding pair of orthogonal basis functions $\phi_{mc}(t)$ and $\phi_{ms}(t)$ for channel m of the demodulator (Figs. 1 and 2) are given by

$$\begin{cases} \phi_{mc}(t) = \sqrt{\frac{2}{T_S}}\cos\left[2\pi\left(f_0^{(\lambda)} + m\cdot 2\Delta\right)t\right] \\ \phi_{ms}(t) = \sqrt{\frac{2}{T_S}}\sin\left[2\pi\left(f_0^{(\lambda)} + m\cdot 2\Delta\right)t\right] \end{cases} \tag{3}$$

where $\lambda = \lfloor t/T_S \rfloor$.

III. Analysis

As shown in Fig. 1, the random variable R_m, $m = 0, 1, \ldots, M-1$, represents the output of the mth channel of the demodulator and is the subtraction of the square-roots of two sums, given by

$$\begin{aligned} R_m =& R_{ma} - R_{mb} \\ =& \sqrt{X_{mca}^2 + X_{msa}^2} - \sqrt{X_{mcb}^2 + X_{msb}^2} \end{aligned} \tag{4}$$

where

$$X_{mca} = \int_0^{T_S} r(t)\phi_{mc}(t)dt, \tag{5}$$

$$X_{msa} = \int_0^{T_S} r(t)\phi_{ms}(t)dt, \tag{6}$$

$$X_{mcb} = \int_0^{\varepsilon T_S} r(t+T_S)\phi_{mc}(t)dt + \int_{(1-\varepsilon)T_S}^{T_S} r(t-T_S)\phi_{mc}(t)dt \tag{7}$$

and

$$X_{msb} = \int_0^{\varepsilon T_S} r(t+T_S)\phi_{ms}(t)dt + \int_{(1-\varepsilon)T_S}^{T_S} r(t-T_S)\phi_{ms}(t)dt. \tag{8}$$

The bit error probability of receiver can be obtained by assuming that the desired signal is present in channel 0 of the demodulator (i.e., $b_0^{(\lambda)} = 0$). Since the cases of hit occurred in all M channels of the receiver due to multiaccess interference are assumed independent of each other when the number of active users $K >> 1$, the probability density functions $\{f_{R_m}(r_m)\}$ of random variables $\{R_m\}$ are also independent. Thus, the probability of symbol error is given by

$$\begin{aligned} P_{\mathrm{SE}} =& 1 - \int_0^{\infty} f_{R_0}(r_0)\left[\int_0^{r_0} f_{R_m}(r_m)dr_m\right]^{M-1} dr_0, \\ m =& 1, 2, \ldots, M-1. \end{aligned} \tag{9a}$$

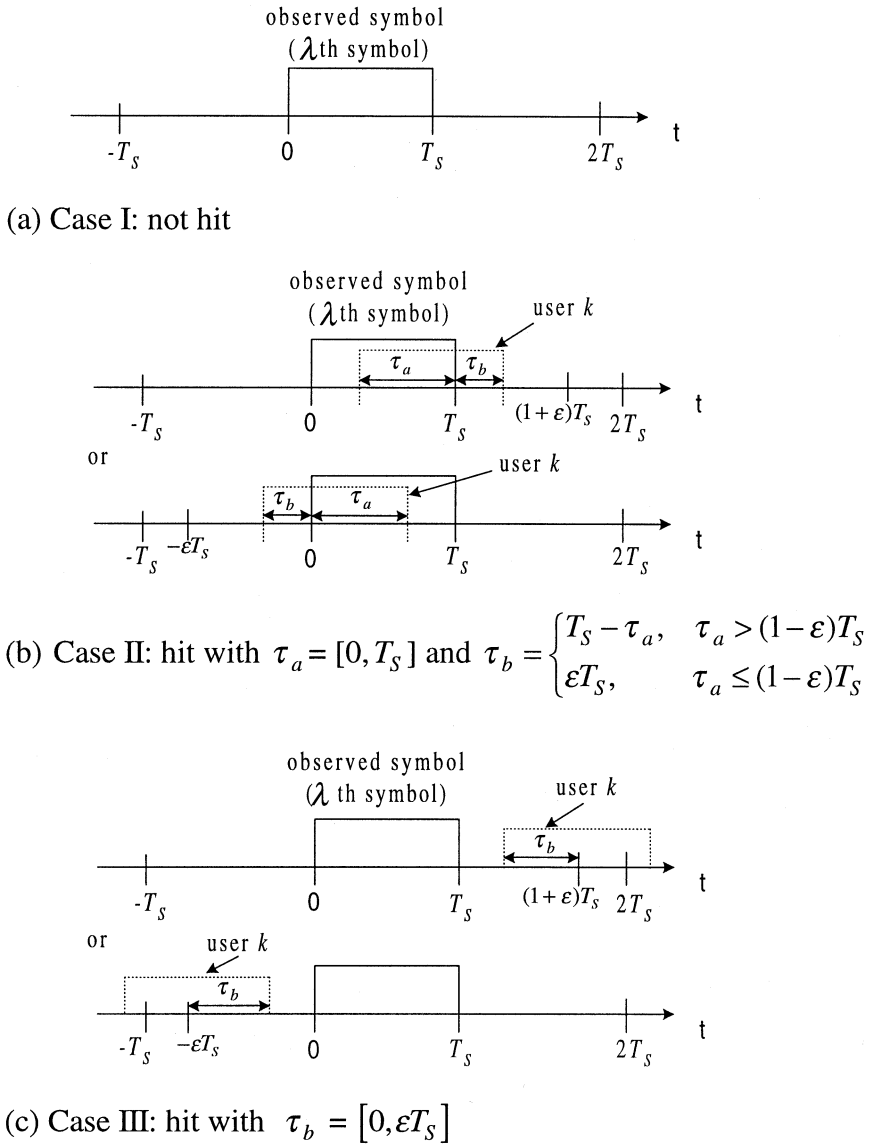

Fig. 3. The cases of hit by user k.

Note that an interference symbol whose delay is less than $-(1+\varepsilon)T_S$ or greater than $(1+\varepsilon)T_S$ does not cause any interference at the output of all correlators due to partial integration (see Fig. 1). In Fig. 3, the time domain is divided into the observed symbol duration

$$A = [0,\ T_S] \tag{9b}$$

and adjacent symbol duration

$$B = [-\varepsilon\, T_S,\ 0] \text{ or } [T_S,\ (1+\varepsilon)T_S]. \tag{9c}$$

In any channel of the receiver, the occurrence of the multiaccess interference can be described in the following three cases. In Case I, channel m is not hit by any nonreference user in duration A and B. In Case II, channel m of the demodulator is hit by a nonreference user (or user k) in duration A and B. The hit duration in duration A is τ_a and hit duration in duration B is τ_b, where τ_a is uniformly distributed in [0, T_S] and $\tau_b = \begin{cases} T_S - \tau_a, & \tau_a > (1-\varepsilon)T_S \\ \varepsilon T_S, & \tau_a \le (1-\varepsilon)T_S \end{cases}$. In Case III, channel m is not hit by a nonreference user in duration A, but is hit in duration B. The hit duration in duration B is τ_b, which is uniformly distributed in [0, $\varepsilon\ T_S$.]

For a large number (Q) of available hopping frequencies, the probability of two or more hits occurred in one of M channels is small. Therefore, we only consider the case that channel m of the reference demodulator is hit by one nonreference user. Two or more hits in one channel at same time are neglected. The probabilities of Cases I, II, and III occurred in one channel of the receiver are given by

$$P_{\text{Case I}} = 1 - \frac{2(1+\varepsilon)(K-1)}{QM} \tag{10a}$$

$$P_{\text{Case II}} = \frac{2(K-1)}{QM} \tag{10b}$$

and

$$P_{\text{Case III}I} = \frac{2\varepsilon(K-1)}{QM} \tag{10c}$$

Since the probability density functions $\{f_{R_m}(r_m)\}$ are independent of each other, $f_{R_m}(r_m)$ can be obtained by averaging over all cases of hit occurred in channel m

$$\begin{aligned} f_{R_m}(r_m) =& P_{\text{Case I}} \cdot f_{R_m|\text{Case I}}(r_m) \\ &+ P_{\text{Case II}} \cdot \frac{1}{T_S}\int_0^{T_S} f_{R_m|\text{Case II}}(r_m|\tau_a)d\tau_a \\ &+ P_{\text{Case III}I} \cdot \frac{1}{\varepsilon T_S}\int_0^{\varepsilon T_S} f_{R_m|\text{Case III}I}(r_m|\tau_b)d\tau_b \end{aligned} \tag{11}$$

where $f_{R_m|\text{Case I}}(r_m)$, $f_{R_m|\text{Case II}}(r_m|\tau_a)$ and $f_{R_m|\text{Case III}}(r_m|\tau_b)$ are the conditional probability density functions of R_m, conditioned on the hit Case I, II, and III, respectively, and are discussed and derived in the following.

1) Case I:

In Sase I, channel m is not hit by any nonreference user. The random variables X_{mca} and X_{msa} in (5) and (6) are given by (12) and (13) shown at the bottom of the page where $\delta(m,0) = 1$ and 0 for $m = 0$ and $m \neq 0$, respectively. Since the two terms on the right hand side of (12) or (13) are Gaussian, both X_{mca} and X_{msa} are Gaussian random variables with the same variance

$$\sigma_{ma}^2 = \sigma_0^2\delta(m,0) + \sigma_N^2 \tag{14}$$

where $\sigma_0^2 = (1/4)E\left[\beta_0^2\right]T_S = P_S T_S/2$ and $\sigma_N^2 = N_0/2$. Therefore, the output of the square root $R_{ma} = \sqrt{X_{mca}^2 + X_{msa}^2}$ is a Rayleigh random variable with the following probability density function:

$$f_{R_{ma}|\text{Case I}}(r_a) = \begin{cases} \frac{r_a}{\sigma_{ma}^2}\exp\left(-\frac{r_a^2}{2\sigma_{ma}^2}\right), & r_a \geq 0 \\ 0, & r_a < 0 \end{cases}. \tag{15}$$

From (7) and (8), X_{mcb} and X_{msb} are given by (16) and (17) shown at the bottom of the page where both X_{mcb} and X_{msb} are zero mean Gaussian random variables with variance

$$\sigma_b^2 = 2\varepsilon\sigma_N^2. \tag{18}$$

Therefore, $R_{mb} = \sqrt{X_{mcb}^2 + X_{msb}^2}$ is a Rayleigh random variable with the following probability density function

$$f_{R_{mb}|\text{Case I}}(r_b) = \begin{cases} \frac{r_b}{\sigma_b^2}\exp\left(-\frac{r_b^2}{2\sigma_b^2}\right), & r_b \geq 0 \\ 0, & r_b < 0 \end{cases}. \tag{19}$$

The probability density function of the mth channel output ($R_m = R_{ma} - R_{mb}$) is convolution between (15) and (19),

$$f_{R_m|\text{Case I}}(r) = \begin{cases} \int_0^\infty f_{R_{ma}|\text{Case I}}(x+r)f_{R_{mb}|\text{ Case I}}(x)dx, & r \geq 0 \\ \int_0^\infty f_{R_{ma}|\text{Case I}}(x)f_{R_{mb}|\text{Case I}}(x-r)dx, & r < 0 \end{cases}. \tag{20}$$

$$\begin{aligned} X_{mca} =& \int_0^{T_S}\left[\beta_0\sin\left(2\pi f_0^{(\lambda)}t + \theta_0\right)\delta(m,0) + n(t)\right]\cdot\sqrt{\frac{2}{T_S}}\cos\left[2\pi\left(f_0^{(\lambda)} + m\cdot 2\Delta\right)t\right]dt \\ =& \sqrt{\frac{T_S}{2}}\beta_0\sin(\theta_0)\,\delta(m,0) + \int_0^{T_S} n(t)\cdot\sqrt{\frac{2}{T_S}}\cos\left[2\pi\left(f_0^{(\lambda)} + m\cdot 2\Delta\right)t\right]dt \end{aligned} \tag{12}$$

$$\begin{aligned} X_{msa} =& \int_0^{T_S}\left[\beta_0\sin\left(2\pi f_0^{(\lambda)}t + \theta_0\right)\delta(m,0) + n(t)\right]\cdot\sqrt{\frac{2}{T_S}}\sin\left[2\pi\left(f_0^{(\lambda)} + m\cdot 2\Delta\right)t\right]dt \\ =& \sqrt{\frac{T_S}{2}}\beta_0\cos(\theta_0)\,\delta(m,0) + \int_0^{T_S} n(t)\cdot\sqrt{\frac{2}{T_S}}\sin\left[2\pi\left(f_0^{(\lambda)} + m\cdot 2\Delta\right)t\right]dt \end{aligned} \tag{13}$$

$$\begin{aligned} X_{mcb} =& \int_0^{\varepsilon T_S} n(t+T_S)\cdot\sqrt{\frac{2}{T_S}}\cos\left[2\pi\left(f_0^{(\lambda)} + m\cdot 2\Delta\right)t\right]dt \\ &+ \int_{(1-\varepsilon)T_S}^{T_S} n(t-T_S)\cdot\sqrt{\frac{2}{T_S}}\cos\left[2\pi\left(f_0^{(\lambda)} + m\cdot 2\Delta\right)t\right]dt \end{aligned} \tag{16}$$

$$\begin{aligned} X_{msb} =& \int_0^{\varepsilon T_S} n(t+T_S)\cdot\sqrt{\frac{2}{T_S}}\sin\left[2\pi\left(f_0^{(\lambda)} + m\cdot 2\Delta\right)t\right]dt \\ &+ \int_{(1-\varepsilon)T_S}^{T_S} n(t-T_S)\cdot\sqrt{\frac{2}{T_S}}\sin\left[2\pi\left(f_0^{(\lambda)} + m\cdot 2\Delta\right)t\right]dt \end{aligned} \tag{17}$$

Substituting (15) and (19) into (20), one obtains (21) shown at the bottom of the page where $\mathrm{erfc}(x) = 2/\sqrt{\pi}\int_x^\infty e^{-t^2}dt$.

2) Case II:

In Case II, channel m is hit by one nonreference user (user k) during the observed symbol period and the hit duration τ_a is uniformly distributed in [0, T_S]. In this case, the same interference user (β_k) may cause interference for both R_{ma} and R_{mb}. From (7) and (8), the random variables X_{mca} and X_{msa} are given by

$$X_{mca} = \sqrt{\frac{T_S}{2}}\beta_0 \sin(\theta_0)\,\delta(m,0) + \frac{\tau_a}{\sqrt{2T_S}}\beta_k \sin(\theta_{ak}) + \int_0^{T_S} n(t)\cdot\sqrt{\frac{2}{T_S}}\cos\left[2\pi\left(f_0^{(\lambda)} + m\cdot 2\Delta\right)t\right]dt \quad (22)$$

and

$$X_{msa} = \sqrt{\frac{T_S}{2}}\beta_0 \cos(\theta_0)\,\delta(m,0) + \frac{\tau_a}{\sqrt{2T_S}}\beta_k \cos(\theta_{ak}) + \int_0^{T_S} n(t)\cdot\sqrt{\frac{2}{T_S}}\sin\left[2\pi\left(f_0^{(\lambda)} + m\cdot 2\Delta\right)t\right]dt \quad (23)$$

where β_k represents the amplitude of the interference signal of the kth nonreference user and is the Rayleigh random variable with mean $(\sqrt{\pi/T_S})\sigma_I$, second moment $(4/T_S)\sigma_I^2$, where σ_I^2 is the energy of one interference symbol θ_{ak} is a random variable uniformly distributed in [0, 2π). We define the random variable $Y = (\sqrt{T_S/2})\beta_k$. The probability density function of Y is given by

$$f_Y(y) = \begin{cases} \frac{y}{\sigma_I^2}\exp\left(-\frac{y^2}{2\sigma_I^2}\right), & y \ge 0 \\ 0, & y < 0 \end{cases}. \quad (24)$$

Note that the random variables R_{ma} and R_{mb} are not independent in Case II since one MAI symbols hit both observed symbol duration and its adjacent symbol duration. Hence, the random variables R_{ma} and R_{mb}, conditioned on Y, are analyzed separately. When $Y = y$, both X_{mca} and X_{msa} are Gaussian random variables with mean $(\tau_a/T_S)y\sin(\theta_{ak})$ and $(\tau_a/T_S)y\cos(\theta_{ak})$, respectively. Therefore, R_{ma} is a Ricean random variable with the pdf

$$f_{R_{ma}|\mathrm{Case\,II}}(r_a|\{\tau_a, y\}) = \begin{cases} \frac{r_a}{\sigma_{ma}^2}\exp\left(-\frac{r_a^2+\left(\frac{\tau_a y}{T_S}\right)^2}{2\sigma_{ma}^2}\right)\cdot I_0\left(\frac{\tau_a y r_a}{T_S\sigma_{ma}^2}\right), & r_a \ge 0 \\ 0, & r_a < 0 \end{cases} \quad (25)$$

where variance σ_{ma}^2 is defined in (14). On the other hand, the random variables X_{mcb} and X_{msb} are given by (26) and (27) shown at the bottom of the page where $\tau_b = \begin{cases} T_S - \tau_a, & \tau_a > (1-\varepsilon)T_S \\ \varepsilon T_S, & \tau_a \le (1-\varepsilon)T_S \end{cases}$. θ_{bk} is a random variable uniformly distributed in [0, 2π). When $Y = y$

$$f_{R_m|\mathrm{Case\,I}}(r) = \begin{cases} \frac{\sigma_{ma}^2 r}{\left(\sigma_{ma}^2+\sigma_b^2\right)^2}\exp\left(-\frac{r^2}{2\sigma_{ma}^2}\right) + \frac{\sqrt{\pi}\sigma_{ma}\sigma_b}{\sqrt{2\left(\sigma_{ma}^2+\sigma_b^2\right)^3}}\left(1-\frac{r^2}{\sigma_{ma}^2+\sigma_b^2}\right) \\ \cdot\exp\left(-\frac{r^2}{2(\sigma_{ma}^2+\sigma_b^2)}\right)\cdot\mathrm{erfc}\left(\sqrt{\frac{\sigma_b}{2(\sigma_{ma}^2+\sigma_b^2)\sigma_{ma}^3}}\cdot r\right), & r \ge 0 \\ \frac{\sigma_b^2(-r)}{\left(\sigma_{ma}^2+\sigma_b^2\right)^2}\exp\left(-\frac{r^2}{2\sigma_{ma}^2}\right) + \frac{\sqrt{\pi}\sigma_{ma}\sigma_b}{\sqrt{2\left(\sigma_{ma}^2+\sigma_b^2\right)^3}}\left(1-\frac{r^2}{\sigma_{ma}^2+\sigma_b^2}\right) \\ \cdot\exp\left(-\frac{r^2}{2(\sigma_{ma}^2+\sigma_b^2)}\right)\cdot\mathrm{erfc}\left(\sqrt{\frac{\sigma_{ma}}{2(\sigma_{ma}^2+\sigma_b^2)\sigma_b^3}}\cdot(-r)\right), & r < 0 \end{cases} \quad (21)$$

$$X_{mcb} = \frac{\tau_b}{\sqrt{2T_S}}\beta_k \sin(\theta_{bk}) + \int_0^{\varepsilon T_S} n(t+T_S)\cdot\sqrt{\frac{2}{T_S}}\cos\left[2\pi\left(f_0^{(\lambda)} + m\cdot 2\Delta\right)t\right]dt + \int_{(1-\varepsilon)T_S}^{T_S} n(t-T_S)\cdot\sqrt{\frac{2}{T_S}}\cos\left[2\pi\left(f_0^{(\lambda)} + m\cdot 2\Delta\right)t\right]dt \quad (26)$$

$$X_{msb} = \frac{\tau_b}{\sqrt{2T_S}}\beta_k \cos(\theta_{bk}) + \int_0^{\varepsilon T_S} n(t+T_S)\cdot\sqrt{\frac{2}{T_S}}\sin\left[2\pi\left(f_0^{(\lambda)} + m\cdot 2\Delta\right)t\right]dt + \int_{(1-\varepsilon)T_S}^{T_S} n(t-T_S)\cdot\sqrt{\frac{2}{T_S}}\sin\left[2\pi\left(f_0^{(\lambda)} + m\cdot 2\Delta\right)t\right]dt \quad (27)$$

, the random variables X_{mcb} and X_{msb} are Gaussian random variables with mean $(\tau_b/T_S)y\sin(\theta_{bk})$ and $(\tau_b/T_S)y\cos(\theta_{bk})$, respectively. Similarly, R_{mb} is also a Ricean random variable with pdf

$$f_{R_{mb}|\text{Case II}}(r_b|\{\tau_a,y\}) = \begin{cases} \frac{r_b}{\sigma_b^2}\exp\left(-\frac{r_b^2+\left(\frac{\tau_b y}{T_S}\right)^2}{2\sigma_b^2}\right)\cdot I_0\left(\frac{\tau_b y r_b}{T_S\sigma_b^2}\right), & r_b\geq 0 \\ 0, & r_b<0 \end{cases} \quad (28)$$

where variance σ_b^2 is defined as (18). Furthermore, we average $f_{R_m|\text{Case II}}(r|\{\tau_a,y\})$ over Y to obtain

$$f_{R_m|\text{CaseII}}(r|\tau_a) = \int_0^\infty f_Y(y) f_{R_m|\text{Case II}}(r|\{\tau_a,y\})\,dy. \quad (29)$$

For $R_m = R_{ma} - R_{mb}$, see (30) at the bottom of the page. Substituting (24), (25) and (28) into (30) and using [13, eq. (6.633.4)], (30) can be simplified as (31) shown at the bottom of the page where $\Psi = \tau_a^2\sigma_b^2\sigma_I^2 + \tau_b^2\sigma_{ma}^2\sigma_I^2 + T_S^2\sigma_{ma}^2\sigma_b^2$.

3) Case III:

In Case III, channel m is not hit by an nonreference user during the observed symbol period, but is hit during the adjacent symbol of the observed signal symbol. The hit duration τ_b is uniformly distributed in [0, εT_S]. In this case, the random variables X_{mca} and X_{msa} are the same as that in Case I, and the random variables X_{mca} and X_{msa} are same as (26) and (27) in Case II but with τ_b uniformly distributed on $[0,\varepsilon T_S]$ (see Fig. 3). Since both X_{mca} and X_{msa} do not include common multiple access interference unlike (22) and (23) in Case II, $\{X_{mca}, X_{msa}\}$ are independent of $\{X_{mca}, X_{msa}\}$. The pdf of R_{ma} is given by (15). However, given τ_b, since both X_{mca} and X_{msb} are Gaussian random variables with variance

$$\hat{\sigma}_b^2(\tau_b) = \left(\frac{\tau_b}{T_S}\sigma_I\right)^2 + 2\varepsilon\sigma_N^2 \quad (32)$$

whereas the pdf of R_{mb} is a Rayleigh distribution, given by (19) with the substitution of σ_b^2 by $\hat{\sigma}_b^2(\tau_b)$. Furthermore, given τ_b, the pdf $f_{R_m|\text{Case III}}(r|\tau_b)$ of R_m in Case III is given by (21) with the substitution of $\hat{\sigma}_b^2$ by $\hat{\sigma}_b^2(\tau_b)$ shown in (33) at the bottom of the page.

Finally, substituting (10), (21), (31) and (33) into (11), we can obtain the average pdf $f_{R_m}(r)$ of random variable R_m, and obtain the uncoded symbol error probability P_{SE} by (9). Once P_{SE} after hard decision has been obtained, assuming symbol errors are random when interleaving technique is used, the corresponding bit error rate (BER) P_{BE} after hard decision is given by

$$P_{BE} = \frac{\frac{M}{2}}{M-1}P_{SE}. \quad (34)$$

Reed–Solomon (RS) codes are nonbinary, linear, cyclic symbol-error-correcting block codes. The length of an RS code is $n = M-1$ M-ary symbols, l of which are redundancy symbols; l can be chosen between 1 and $M-2$. In this paper, we select $l = (M-2)/2$ so that the coding rate l/n is nearly 1/2, and the code can correct up to $t = M/4$ symbol errors. When decoding of RS codes with hard decision is employed,

$$f_{R_m|\text{Case II}}(r|\tau_a) = \begin{cases} \int_0^\infty f_Y(y)\int_0^\infty f_{R_{ma}|\text{Case II}}(x+r|\{\tau_a,y\})\,f_{R_{mb}|\text{Case II}}(x|\{\tau_a,y\})dxdy, & r\geq 0 \\ \int_0^\infty f_Y(y)\int_0^\infty f_{R_{ma}|\text{Case II}}(x|\{\tau_a,y\})\,f_{R_{mb}|\text{Case II}}(x-r|\{\tau_a,y\})\,dxdy, & r<0. \end{cases} \quad (30)$$

$$f_{R_m|\text{Case II}}(r|\tau_a) = \begin{cases} \frac{T_S^2}{\Psi}\int_0^\infty x(x+r)\exp\left(-\frac{x^2\left(\tau_a^2\sigma_I^2+T_S^2\sigma_{ma}^2\right)+(x+r)^2\left(\tau_b^2\sigma_I^2+T_S^2\sigma_b^2\right)}{2\Psi}\right) & \\ \cdot I_0\left(\frac{x(x+r)\tau_a\tau_b\sigma_I^2}{\Psi}\right)dx, & r\geq 0 \\ \frac{T_S^2}{\Psi}\int_0^\infty x(x-r)\exp\left(-\frac{(x-r)^2\left(\tau_a^2\sigma_I^2+T_S^2\sigma_{ma}^2\right)+x^2\left(\tau_b^2\sigma_I^2+T_S^2\sigma_b^2\right)}{2\Psi}\right) & \\ \cdot I_0\left(\frac{x(x-r)\tau_a\tau_b\sigma_I^2}{\Psi}\right)dx, & r<0 \end{cases} \quad (31)$$

$$f_{R_m|\text{Case III}}(r|\tau_b) = \begin{cases} \frac{\sigma_{ma}^2 r}{\left(\sigma_{ma}^2+\hat{\sigma}_b^2\right)^2}\exp\left(-\frac{r^2}{2\sigma_{ma}^2}\right) + \frac{\sqrt{\pi}\sigma_{ma}\hat{\sigma}_b}{\sqrt{2\left(\sigma_{ma}^2+\hat{\sigma}_b^2\right)^3}}\left(1-\frac{r^2}{\sigma_{ma}^2+\hat{\sigma}_b^2}\right) & \\ \cdot\exp\left(-\frac{r^2}{2(\sigma_{ma}^2+\hat{\sigma}_b^2)}\right)\cdot\text{erfc}\left(\sqrt{\frac{\hat{\sigma}_b}{2(\sigma_{ma}^2+\hat{\sigma}_b^2)\sigma_{ma}^3}}\cdot r\right), & r\geq 0 \\ \frac{-\hat{\sigma}_b^2 r}{\left(\sigma_{ma}^2+\hat{\sigma}_b^2\right)^2}\exp\left(-\frac{r^2}{2\sigma_{ma}^2}\right) + \frac{\sqrt{\pi}\sigma_{ma}\hat{\sigma}_b}{\sqrt{2\left(\sigma_{ma}^2+\hat{\sigma}_b^2\right)^3}}\left(1-\frac{r^2}{\sigma_{ma}^2+\hat{\sigma}_b^2}\right) & \\ \cdot\exp\left(-\frac{r^2}{2(\sigma_{ma}^2+\hat{\sigma}_b^2)}\right)\cdot\text{erfc}\left(\sqrt{\frac{\sigma_{ma}}{2(\sigma_{ma}^2+\hat{\sigma}_b^2)\hat{\sigma}_b^3}}\cdot(-r)\right), & r<0. \end{cases} \quad (33)$$

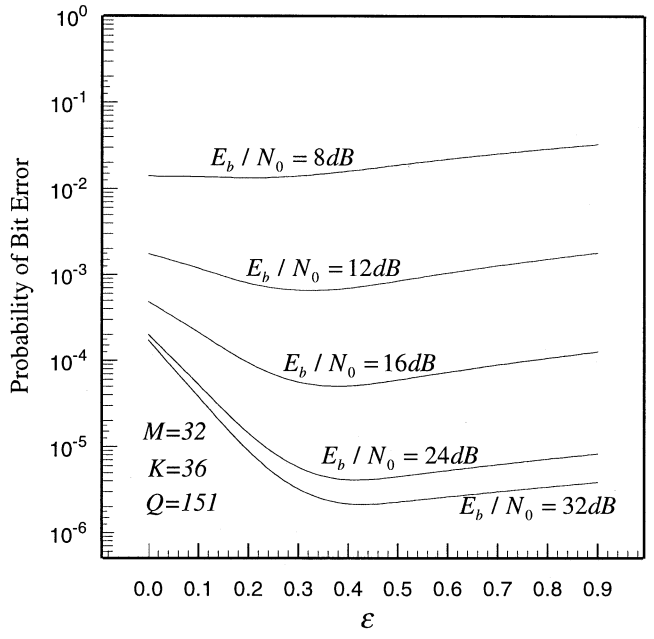

Fig. 4. The probability of bit error versus the parameter with RS coding.

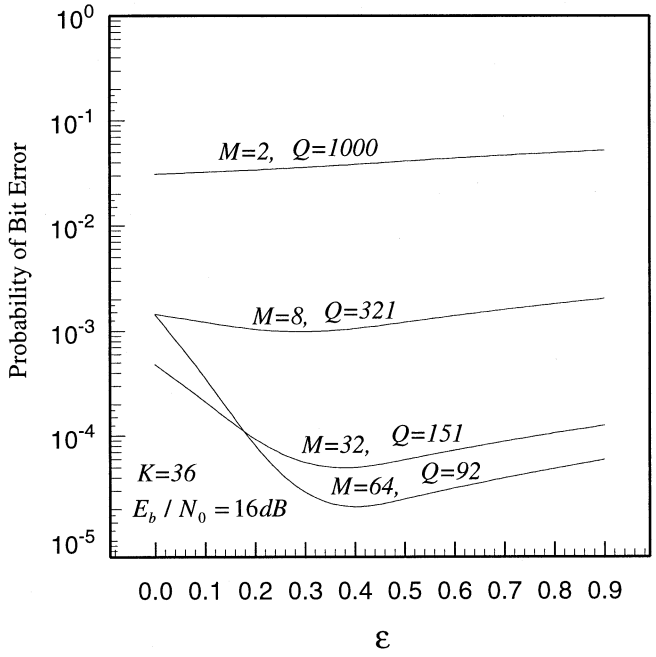

Fig. 5. The probability of bit error versus the parameter with RS coding.

the symbol error probability P_{SEC} after RS decoding is well approximated by [6]

$$P_{\mathrm{SEC}} = \frac{1}{n} \sum_{j=t+1}^{n} j \begin{bmatrix} n \\ j \end{bmatrix} [P_{\mathrm{SE}}]^j [1 - P_{\mathrm{SE}}]^{n-j} \qquad (35)$$

where $t = M/4$ and $n = M-1$. The BER P_{SEC} after decoding is approximated by substituting in (34) P_{BE} and P_{SE} by P_{BEC} and P_{SEC}.

IV. Numerical Results

The probability of bit error of the novel MFSK receiver in a FHMA system with the Rayleigh-fading channel is now numerically computed. For fair comparison, all of the following results are obtained under the condition that $W_{\mathrm{Total}}/R_i = Q\,(M/\log_2 M)\,(n/l) = 2000$ is fixed where $(n/l) \approx 0.5$ for coding.

First, the effects of the parameter ε of the additional partial correlators on the performance of the MFSK receiver are shown in Figs. 4 and 5. The probability of bit error is shown in Fig. 4 for various values of E_b/N_0 when the modulation order $M = 32$, whereas it is shown in Fig. 5 for various values of M when $E_b/N_0 = 16$ dB. Note that the performance of a conventional receiver is shown in the both figures when $\varepsilon = 0$. It can be seen from Fig. 4 that when $E_b/N_0 = 8$ dB, the performance of a conventional receiver is better. However, when E_b/N_0 is large, i.e., $E_b/N_0 \geq 12$ dB, the performance of a novel receiver is better. The probability of bit error decreases when ε increases for a given value of E_b/N_0. When ε takes an optimum value ($\varepsilon \approx 0.4$), the error probability reaches the minimum. When ε keeps increasing after the optimum value, the probability of error steadily increases. The optimum value of ε is a function of E_b/N_0, but it falls in the region from approximately 0.3 to 0.5. The optimum region of ε from 0.3 to 0.5 can also be observed in Fig. 5 when $M \geq 8$. Note that in the novel receiver, the MAI

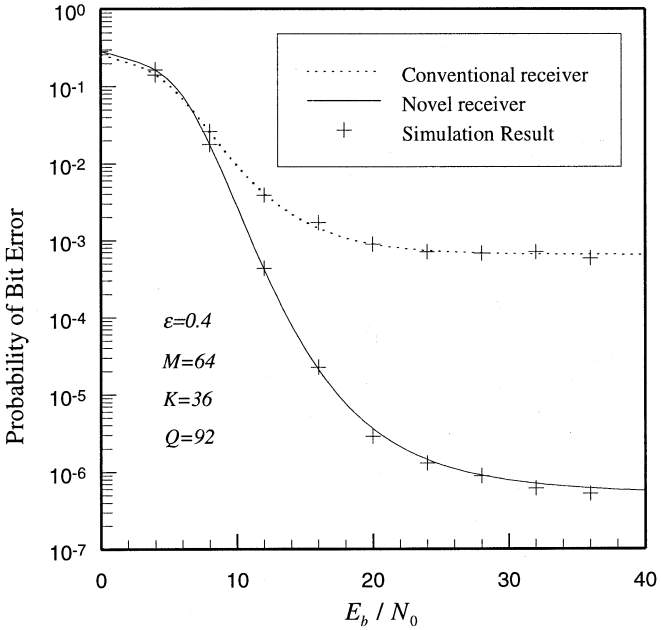

Fig. 6. The probability of bit error with RS coding.

can be reduced in the subtraction of R_{ma} and R_{mb} in the Case II. For the Cases I and III, however, the use of additional partial correlators introduce more noise. The noise increases when ε increases. Thus, an optimum value of ε exists. When E_b/N_0 reduces, the noise energy increases and optimum value of ε decreases. On the other hand, when the channel m is hit by a MAI tone, the use of additional partial correlators reduces the output of channel m. If the channel m is signal channel, the additional partial correlators are destructive to the performance. The probability that the signal channel is hit is $1/M$. This is the reason when the modulation order M is larger, the effect of the novel receiver is better, and the optimum value of ε also increases.

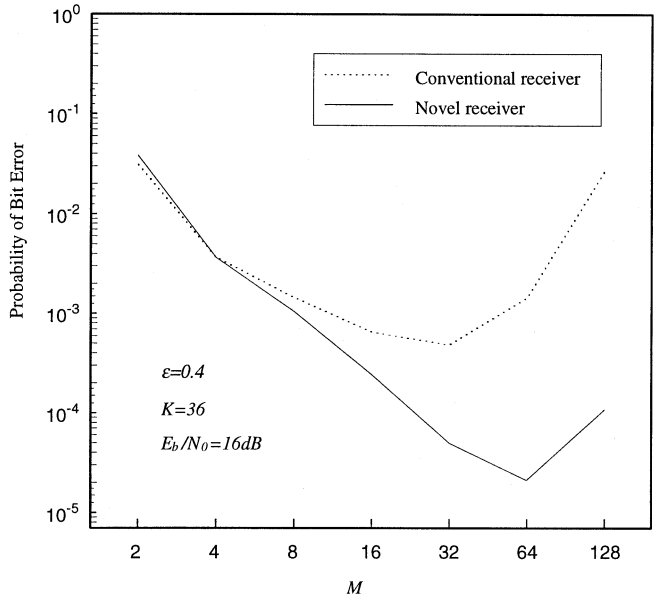

Fig. 7. The probability of bit error versus the modulation order M with RS coding.

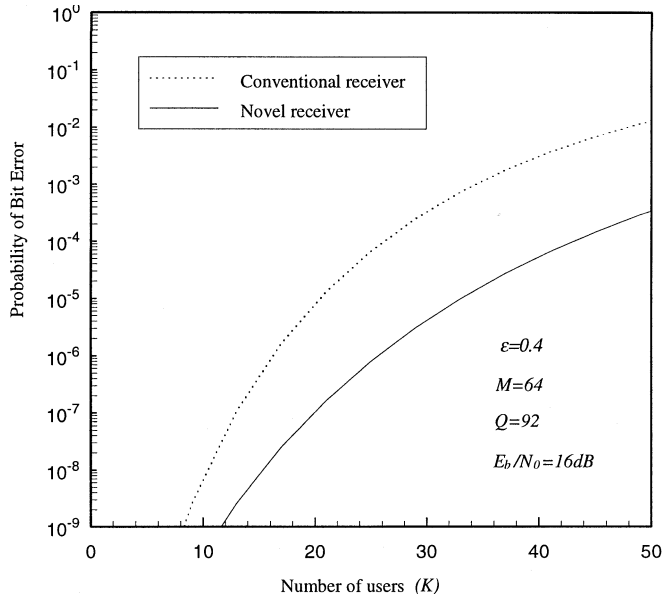

Fig. 8. The probability of bit error with RS coding.

It can also be seen from the both figures that given E_b/N_0 or M, the performance is not very sensitive to ε when ε takes any value from the region of 0.3 to 0.5. Therefore, the medium value of $\varepsilon = 0.4$ is used for following figures.

The BER performance of the novel and conventional receiver is plotted in Fig. 6 as a function of E_b/N_0 when the modulation order $M = 64$. The simulation result is also shown for comparison. It can be seen that when E_b/N_0 is small, the performance of a novel receiver is slightly poorer than that of a conventional receiver since the white noise dominates the multiple access interference. However, when E_b/N_0 is large, the multiple access interference dominates so that the novel receiver is better because it uses the side information of the interfering signal to reduce the interference. When E_b/N_0 is very large, the significant improvement in performance has been achieved with the novel receiver. It can be seen from this figure that the analytical results are very close to simulation results so that our analytic results are very valid.

Fig. 7 illustrates the BER for both receivers as a function of modulation order M. It can be seen that when $M \leq 4$, the conventional receiver performances better than novel receiver. However, when $M > 4$, the novel receiver is better. For a fixed system bandwidth, the best performance is achieved when $M = 32$ for a conventional receiver, while the optimum value of M is 64 for a novel receiver. Actually, this is consistent with Fig. 5. When M is larger than the optimum value, the performance degrades.

Finally, the BER is shown in Fig. 8 as a function of number of active users (K). It can be seen that for a BER of 10^{-4}, the system capacity with novel receivers is almost as twice as that with conventional receivers.

V. Conclusion

In this paper, the performance of the novel FHMA/MFSK receiver has been investigated. The following conclusions have been drawn:

1) the novel receiver performs much better than a conventional receiver for a wide range of signal to noise ratio;
2) the optimum value of parameter ε of the partial correlators in the novel receiver is in the region of 0.3 to 0.5;
3) for a fixed system bandwidth, the optimum modulation order M is 64 for novel receivers, while the optimum M is 32 for conventional receivers;
4) the capacity of the system with novel receivers is almost twice as that of the system with conventional receivers.

Acknowledgment

The authors would like to thank the Research Grant Council (RGC) of the Hong Kong Government and the CRCG of the University of Hong Kong.

References

[1] A. S. Park, R. M. Buehrer, and B. D. Woerner, "Thoughput performance of an FHMA system with variable rate coding," *IEEE Trans. Commun.*, vol. 46, pp. 521–532, Apr. 1998.
[2] J. Wang and M. Moeneclaey, "Multiple hopes/symbol FFH-SSMA with MFSK modulation and Reed–Solomon coding for indoor radio," *IEEE Trans. Commun.*, vol. 41, no. 5, pp. 793–807, May 1993.
[3] J. Ilow, D. Hatzinakos, and A. N. Venetsanopoulos, "Performance of FH SS radio networks with interference modeled as a mixture of Gaussian and Alpha-Stable Noise," *IEEE Trans. Commun.*, vol. 46, pp. 509–519, Apr. 1998.
[4] M. Hegde and W. E. Stark, "Capacity of frequency-hop spread-spectrum multiple-access communication systems," *IEEE Trans. Commun.*, vol. 38, pp. 1050–1059, July 1990.
[5] A. Rahman and A. K. Elhakeem, "Concatenated combined modulation and coding of frequency Hopping multiaccess systems," *IEEE J. Select. Areas Commun.*, vol. 8, pp. 650–662, May 1990.
[6] A. A. M. Saleh and L. J. Cimini, "Indoor radio communications using time-division multiple access with cyclical slow frequency hopping and coding," *IEEE J. Select. Areas Commun.*, vol. SAC-7, pp. 59–70, 1989.
[7] M. A. Wickert and R. L. Turcotte, "Probability of error analysis for FHSS/CDMA communications in the presence of fading," *IEEE J. Select. Areas Commun.*, vol. 10, pp. 523–534, Apr. 1992.
[8] S. W. Kim and W. Stack, "Optimum rate Reed–Solomon Codes for requency-hopped spread-spectrum multiple-access communication systems," *IEEE Trans. Commun.*, vol. 37, pp. 138–144, Feb. 1989.

[9] E. Geraniotis, "Multiple-Access capability of frequency-hopped spread-spectrum revisited: An analysis of the effect of unequal power levels," *IEEE Trans. Commun.*, vol. 38, pp. 1066–1077, July 1990.
[10] K. Cheun and W. Stark, "Probability of error in frequency-hop spread-spectrum multiple-access communication systems with noncoherent reception," *IEEE Trans. Commun.*, vol. 39, no. 9, pp. 1400–1409, Sept. 1991.
[11] Y.-R. Tsai and J.-F. Chang, "Using frequency hopping spread spectrum technique to combat multipath interference in a multiaccessing environment," *IEEE Trans. Veh. Technol.*, vol. 43, pp. 211–222, May 1994.
[12] D. B. Brick and F. W. Ellersick, "Future air force tactical communications," *IEEE Trans. Commun.*, vol. COM-28, pp. 1551–11 572, Sept. 1980.
[13] I. S. Gradshteyn and I. M. Ryzhik, *Table of Integration, Series and Productions*, 5nd ed. New York: Academic, 1996.

Chen Jiang received the B.S. and M.S. degree from Southeast University, Nanjing, China, in 1985 and 1988, respectively, and the Ph.D. degree from the University of Hong Kong, China, in 2000, all in electronic engineering.

From 1988 to 1996, he was with the Communication Department, Nanjing Automation Institute, as a Firmware Engineer. Since 2000, he has been a Senior Hardware Design Engineer with Nortel Networks, Ottawa, ON, Canada, where he works on the research and development of the OC-192 Ultra-Long Reach optical communication system.

Jiangzhou Wang (M'91–SM'94) received the B.S. and M.S. degrees from Xidian University, Xian, China, in 1983 and 1985, respectively, and the Ph.D. degree (with greatest distinction) from the University of Ghent, Belgium, in 1990, all in electrical engineering.

From 1990 to 1992, he was a Postdoctoral Fellow at the University of California at San Diego, where he worked on the research and development of cellular CDMA systems. From 1992 to 1995, he was a Senior System Engineer with Rockwell International Corporation, Newport Beach, CA, where he worked on the development and system design of wireless communications. Since 1995, he has been with the University of Hong Kong, China, where he is currently a Coordinator of Telecommunications and an Associate Professor. He has held a Visiting Professor position with NTT DoCoMo, Japan. He has written/edited two books: *Broadband Wireless Communications* (Norwell, MA: Kluwer, 2001) and *Advances in 3G Enhanced Technologies for Wireless Communications* (Norwood, MA: Artech House, 2002). He has received one U.S. patent related to the GSM system. He has published more than 100 papers n the areas of wireless mobile and spread-spectrum communications.

Dr. Wang is an Editor for the IEEE TRANSACTIONS ON COMMUNICATIONS and a Guest Editor for the IEEE JOURNAL ON SELECTED AREAS IN COMMUNICATIONS. He was a Technical Chairman of IEEE Workshop in 3G Mobile Communications, 2000. His publications include more than 20 IEEE TRANSACTIONS/JOURNAL papers. He is listed in *Who's Who in the World.*